Biochimica et Biophysica Acta, 943 (1988) 63–75
Elsevier

BBA 74065

Phase metastability and supercooled metastable state of diundecanoylphosphatidylethanolamine bilayers *

Hui Xu, Frances A. Stephenson, Hai-nan Lin and Ching-hsien Huang

Department of Biochemistry, University of Virginia School of Medicine, Charlottesville, VA (U.S.A.)

(Received 16 February 1988)

Key words: Phosphatidylethanolamine; Metastability; Phase transition; Cooling; NMR, ^{31}P-; Differential scanning calorimetry

Aqueous dispersons of L-α-phosphatidylethanolamine (PE) with identical saturated acyl chains are known to exhibit gel-state metastability. It is also known that the metastability in PE becomes more pronounced with decreasing acyl chain-length. In an attempt to study the metastable phase behavior of PE, we have synthesized diundecanoylphosphatidylethanolamine ($diC_{11}PE$) and examined its polymorphic phase behavior. A single endothermic transition at 38°C is detected between 10 and 55°C by DSC for the nonheated sample of $diC_{11}PE$ in excess water. An immediate second heating scan done after cooling slowly of the same sample from the liquid-crystalline state shows a smaller endothermic transition at a lower temperature, 18°C. However, the high-temperature transition at 38°C can be detected, if the sample which has been heated above 38°C is quench cooled from the liquid-crystalline to a temperature between 18 and 38°C. Furthermore, two endothermic transitions at 18 and 38°C and an exothermic transition at 19°C are recorded for $diC_{11}PE$ after quench supercooling of the sample from the liquid-crystalline state to an appropriate temperature below 10°C. The gel-state metastability of $diC_{11}PE$ can be most appropriately explained in terms of changes in interbilayer headgroup–headgroup interactions. It is suggested that the kinetically trapped supercooled metastable state may be a multilamellar structure with melted acyl chains but with strong interbilayer headgroup–headgroup interactions.

Introduction

L-α-Phosphatidylethanolamines (PEs) with identical saturated acyl chains are well known to self assemble into lamellae in excess water. When lamellae of PE with a single type of saturated fatty acid composition are heated, a highly cooperative endothermic transition corresponding to the gel to liquid-crystalline (L_α) phase transition occurs. Unlike the main phase transition of phosphatidylcholine (PC) dispersions, the thermotropic behavior of this phase transition depends on the thermal history of the PE sample [1–6]. For instance, an aqueous dispersion of $diC_{12}PE$ which has not been heated above T_m shows a highly cooperative endothermic transition at 44.65°C by DSC on the first heating scan, whereas a second heating scan of the same sample done immediately after cooling from the liquid-crystalline state exhibits an overlapped multicomponent endothermic peak centered at a lower temperature of approx.

* This paper is dedicated to James W. Ogilvie, as an expression of appreciation and gratitude for his scientific and personal qualities, on the occasion of his retirement.

Abbreviations: PC, phosphatidylcholine; PE, phosphatidylethanolamine; $diC_{11}PE$, diundecanoylphosphatidylethanolamine; diC_xPE, saturated diacylphosphatidylethanolamine having x carbons in each of the acyl chains; N-monomethyl-$diC_{11}PE$, 1,2-diundecanoyl-*sn*-glycero-3-phospho-*N*-methylethanolamine; T_m, transition temperature; $\Delta T_{1/2}$, transition peak width at half-height; DSC, differential scanning calorimetry.

Correspondence: C. Huang, Department of Biochemistry, Box 440, University of Virginia School of Medicine, Charlottesville, VA 22908, U.S.A.

30 °C [4]. If the sample which has been heated above T_m is allowed to anneal at a temperature of 4 °C for several days, the high-temperature phase transition will reappear in the thermogram [1]. The dependence of the phase transition behavior on the thermal history of PE dispersions is attributed to the metastability of the gel phase of saturated PE below a certain temperature; the metastable gel state (L_β) reverts slowly but spontaneously to a more stable and less hydrated crystalline state (L_c) at appropriate low temperatures [1–3]. The metastable phase behavior is observed to be chain-length dependent for an homologous series of phospholipids ranging from $diC_{12}PE$ to $diC_{18}PE$ in excess water [4]. The down shifts in T_m observed for lamellar PEs in the second heating scan become progressively smaller as the length of the acyl chain increases, and the magnitude of the shift can be extrapolated to zero at $diC_{20}PE$ [4]. In order to study the metastability of fully hydrated saturated phosphatidylethanolamines, it is thus better to choose the molecular species of PE with shorter acyl chains.

We have synthesized $diC_{11}PE$ and its *N*-monomethyl derivative. We then examined their thermotropic phase behavior by high resolution differential scanning calorimetry. Our calorimetric results indicate that $diC_{11}PE$ displays gel-phase and liquid crystalline-phase metastability under certain experimental conditions and that quick supercooling of $diC_{11}PE$ from the liquid-crystalline phase to an appropriate low temperature results in the occurrence of two endothermic transitions and an exotherm on the subsequent heating scan. Moreover, the gel-phase metastable behavior is eliminated when one of the hydrogen atoms of the ammonium group in the $diC_{11}PE$ headgroup is substituted by a methyl group. In this communication, we propose that hydration/dehydration of lipid headgroup modulates the metastable phase behavior of PE bilayers.

Materials and Methods

Chemicals. Synthetic diundecanoylphosphatidylcholine ($diC_{11}PC$) with purity greater than 99 mol% was supplied by Avanti Polar Lipids (Birmingham, AL). Ethanolamine hydrochloride with purity greater than 99%, and 2-(methylamino)ethanol were obtained from Aldrich (Milwaukee, WI). Phospholipase D, type I from cabbage, was purchased from Sigma (St. Louis, MO). Gaseous HCl was obtained from Matheson Gas Products (E. Rutherford, NJ). Absolute ether with a trace (0.005%) of alcohol was purchased from Curtin Matheson (Jessup, MD); this chemical was further freed of alcohol by column chromatography on alumina prior to use. Other solvents or reagents were of spectral grade or the highest available purity. Water used in the present work was deionized and glass-distilled.

N-Methylethanolamine hydrochloride. Crystalline *N*-methylethanolamine hydrochloride was prepared from aqueous 2-(methylamino)ethanol and HCl as described by Gagné et al. [7]. Briefly, the starting material of aqueous 2-(methylamino) ethanol from Aldrich was purified by fractional distillation under reduced pressure. The freshly distilled sample was collected in a round-bottom flask containing methylene chloride, and the mixture was bubbled with HCl gas. The product, *N*-methylethanolamine hydrochloride, was recrystallized from ethanol at −25 °C. After removing the solvent by reduced pressure and use of a suction, the crystalline compound was dried thoroughly by keeping it under vacuum over P_2O_5 for several days.

N-Monomethylated phosphatidylethanolamine. Diundecanoylphosphatidyl-*N*-methylethanolamine (*N*-methyl-$diC_{11}PE$) was synthesized by the base exchange transphosphatidylation by phospholipase D from the corresponding $diC_{11}PC$ in the presence of excess amount of *N*-methylethanolamine hydrochloride at pH 5.6 according to the method of Comfurius and Zwaal [8]. First, the lyophilized $diC_{11}PC$ was dissolved in absolute diethyl ether (20 mg/ml). The lipid-ether solution was diluted with two volumes of 35% (w/v) *N*-methylethanolamine hydrochloride in aqueous acetate buffer (100 mM, pH 5.6) containing 100 mM $CaCl_2$. Then, the transphosphatidylation was initiated by the addition of crystalline phospholipase D at an enzyme/PC ratio of 1 unit per μmol. If necessary, additional phospholipase D of equal amount was added every 6 h. The base exchange reaction was allowed to proceed for 24 h at room temperature. After the ether had been removed by evaporation on a rotary evaporator, an aliquot of

EDTA (500 mM at pH 8.5), equivalent to 20% by volume of the acetate buffer used, was added into the mixture to chelate Ca^{2+} ions. The mixture was shaken vigorously with 2.2 volume of chloroform/methanol (5:6, w/v) in a separatory funnel, and the lower chloroform phase was collected. The upper phase was extracted one more time with chloroform. The chloroform phases were pooled, and the crude lipid products were dried down from the chloroform. Finally, pure *N*-methylated PEs were isolated by silicic acid column chromatography as described by Gagné et al. [7], and the purity of the final products was evaluated [7].

Diundecanoylphosphatidylethanolamine. The enzymatic synthesis of diundecanoylphosphatidylethanolamine ($diC_{11}PE$) from $diC_{11}PC$ is similar to the one described above for *N*-methyl-$diC_{11}PE$, except that one of the starting materials is crystalline ethanolamine hydrochloride, which can be obtained commercially from Aldrich. This crystalline compound was dissolved in 100 mM acetate buffer (pH 5.6) containing 100 mM $CaCl_2$ to form a 30% (w/v) solution. It was then mixed with the PC-ether solution followed by the base exchange reaction by phospholipase D to form the final product.

Sample preparation. Aqueous lipid dispersions used for DSC experiments were prepared from lyophilized phospholipids rehydrated in 50 mM NaCl solution (0°C) containing 5 mM phosphate buffer and 1 mM EDTA at pH 7.4 to give a final lipid concentration in the range of 2.0–5.5 mM. The exact lipid concentrations were determined by phosphorus analysis [9]. Prior to the DSC experiments, the dispersions were treated in two different ways. One treatment involved the sonication of cold lipid dispersions for 20 min using a bath-type sonicator (Branson Model B-220, 100 watts) filled with ice-water; these are called nonheated samples. A second treatment involved the intermittent sonication of the lipid dispersions on a Branson B-220 sonicator for 3 min under a N_2-atmosphere at 55°C, a temperature well above the higher melting temperature. The sample was then cooled down immediately to 4°C. After incubating for 15 min at 4°C, the sample was heated again to 55°C and then kept at the elevated temperature for 30 min with intermittent sonications. This cooling/heating cycle was repeated two more times. The total duration of intermittent sonications during the repeated cooling/heating cycle of the sample was about 9 min at 55°C under N_2 atmosphere. Finally, the sample was cooled to lower temperatures and stored at the lower temperature for known time intervals prior to DSC experiments. This sample is termed the heat-treated sample. The purity of the sample was checked by thin-layer chromatography, and no degradation was observed.

Quench cooling and quench supercooling. The $diC_{11}PE$ sample with a fixed concentration of 3.04 mM and with a volume of 3 ml was first prepared in a test tube (1.6 × 10 cm). After flushing thoroughly with N_2, the test tube was tightly sealed with screw-cap. The sample was then heated to 55°C followed by intermittent sonications. After immediate cooling of the sample in an ice-water mixture, the heat/intermittent sonication/cooling was repeated twice. For quench cooling experiments, the sample tube at 55°C (or 45°C) was immediately immersed into a circulatory water-bath which had been adjusted to a fixed lower temperature between 18 and 38°C. After incubating at the lower temperature for 45 min with occasional shaking, the sample was degassed and then injected into the sample cell of the calorimeter which had been preequilibrated at the same fixed lower temperature. Prior to the DSC heating run, the sample cell was further thermally equilibrated for 1 h at the fixed temperature. For quench supercooling experiments, the tube containing the heat-treated $diC_{11}PE$ sample in the liquid-crystalline state was immediately placed in the freezer at −40°C. After supercooling at −40°C for various time intervals, the supercooled sample tube was allowed to melt in an ice-water bath. The sample was degassed and then placed into the sample cell of the calorimeter which had been preequilibrated at 0°C. Prior to the DSC heating run, the sample was further incubated in the calorimeter for 1 h at 0°C.

Differential scanning calorimetry (DSC). All DSC measurements were made with a high-resolution MC-2 differential scanning microcalorimeter (Microcal Inc., Amherst, MA). Calorimetric data were collected automatically with the Da-2 digital interface and data acquisition system as described previously [10]. Unless indicated otherwise, all

thermograms were recorded at a nominal heating rate of 10 °C/h. If the sample was rescanned, it was always cooled inside the calorimetric cell after the first heating run. The cooling rate, however, cannot be adjusted in our microcalorimeter; it takes approx. 45 min to lower the temperature of the sample from 55 °C to 0 °C in the microcalorimeter. The transition temperatures and transition enthalpies were determined as described previously [10].

^{31}P-NMR. All proton-decoupled ^{31}P-NMR spectra were obtained at 121 MHz in 10-mm tubes with a General Electric GN300 Fourier transform spectrometer. A fully phase-cycled Hahn echo sequence, as described by Rance and Byrd [11], was used to eliminate spectral distortions. No first-order phase corrections were employed. The decoupler was gated on only during spectral acquisition, following the sequence described by Shaka et al. [12]. Unless indicated otherwise, 8000–10000 transients were accumulated with a 1-s interpulse time. The sample contained 100 mg/ml of diC$_{11}$PE in 50 mM KCl aqueous solution containing 2 mM EDTA, 10 mM piperazine-*N*,*N*-bis-(2-ethanesulfonic acid) and 20% ^2H_2O at pH 7.0. Prior to the NMR measurements, samples were first heated to 55 °C and were vortexed vigorously at the elevated temperature for 2–4 min. Samples were then cooled immediately to 0 °C. After the heating/cooling cycle was repeated two more times, samples were incubated at 0 °C for three days prior to the NMR experiments.

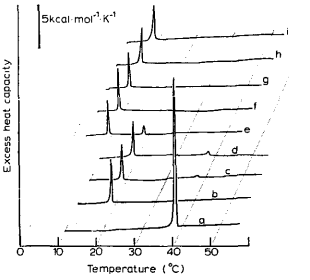

Fig. 1. Successive DSC thermograms of diC$_{11}$PE and *N*-monomethyl-diC$_{11}$PE dispersions. (a) Initial heating scan of a non-heated sample of diC$_{11}$PE, lipid concentration: 3.8 mM; (b) second heating scan following (a); (c) third heating scan after incubating the same sample at 2 °C for 14 h in the calorimeter; (d) second heating scan of a diC$_{11}$PE sample (3.23 mM) which, after cooling from 55 °C to 2 °C in the calorimeter, was incubated at 2 °C for 2 days in the calorimeter prior to the DSC scan. (e) initial heating scan of a nonheated sample of *N*-monomethyl-diC$_{11}$PE, lipid concentration: 2.9 mM; (f) second heating scan following (e); (g) third heating scan after incubating the same sample at 2 °C for 14 h in the calorimeter; (h) second heating scan of a *N*-methyl-diC$_{11}$PE sample (4.00 mM) which, after cooling from 55 °C to 2 °C in the calorimeter, was incubated for 2 days prior to DSC scan; (i) DSC heating thermogram for a heat-treated sample of *N*-methyl-diC$_{11}$PE (4.00 mM). This heat-treated sample was incubated at 2 °C for 9 days to allow full equilibration in the gel state prior to calorimetry.

Results

Thermotropic behavior of diC$_{11}$PE and N-methyl-diC$_{11}$PE dispersions

Fig. 1a shows a representative heating thermogram for nonheated diC$_{11}$PE dispersions obtained in the temperature range of 10 to 55 °C. The heating scan of the nonheated sample exhibits a single sharp endothermic transition with a transition peak width at half-height ($\Delta T_{1/2}$) of 0.48 ± 0.05 °C; this transition, designated as the G(I) → L_α phase transition, is centered at 38.37 ± 0.05 °C with a calorimetric enthalpy (ΔH) of 13.96 ± 1.00 kcal/mol (Fig. 1a). After the first scan, the sample was cooled in the calorimeter cell from 55 °C to 10 °C. Prior to the second heating run, a thermal equilibration time of about 1 h at 10 °C was allowed for the sample. The second heating scan of diC$_{11}$PE dispersions is shown in Fig. 1b, which is characterized again by a single sharp endothermic transition with $\Delta T_{1/2}$ of 0.38 °C; however, this transition is now shifted to a lower temperature centered at 18.64 °C with a considerably smaller value of ΔH (2.86 kcal/mol) (Fig. 1b). Subsequent repeated heating scans of the same sample after cooling to 10 °C in the calorimeter show thermotropic behavior similar to that of the second heating run as shown in Fig. 1b, and we assign this transition as the G(II) → L_α phase transition. However, if the sample, after cooling from 55 °C, is incubated in the calorimeter for a

prolonged time at temperatures below 10°C, it displays two endotherms corresponding to the $G(I) \rightarrow L_\alpha$ and $G(II) \rightarrow L_\alpha$ transitions on the succeeding heating scan. Figs. 1c and 1d show the repeated heating scans of $diC_{11}PE$ dispersions after incubating in the calorimeter at 2°C for 14 h and 2 days, respectively. These thermograms show two discernible endotherms with maxima occurring at 18.6 and 38.4°C, respectively. It is thus clear that with prolonged incubation at 2°C there is a slow reappearance of the high-temperature transition at 38.4°C. Hence, the sample of $diC_{11}PE$ displays metastability of the G(II) phase after prolonged incubation at low temperatures.

We have also examined the thermotropic phase behavior of *N*-methyl-$diC_{11}PE$, in excess water, by high resolution DSC. The initial heating thermogram of the nonheated sample in the temperature range of 2–45°C shows two endothermic transitions. The low-temperature endotherm is centered at 9.1°C with $\Delta H = 1.8$ kcal/mol and $\Delta T_{1/2} = 0.26$ C° while the high-temperature one is at 18.4°C with $\Delta H = 0.69$ kcal/mol and $\Delta T_{1/2} = 0.43$ C° (Fig. 1e). After cooling to 2°C and equilibration for 1 h at 2°C in the calorimeter, an immediate second heating run results in an endothermic transition, shown in Fig. 1f, which is characterized by a single peak centered at $T_m = 9.1 \pm 0.1$°C with $\Delta H = 2.0 \pm 0.3$ kcal/mol and $\Delta T_{1/2} = 0.25 \pm 0.02$ C°. This transition corresponds to the low-temperature transition observed in Fig. 1e. After the second heating scan, the sample was cooled to 2°C and incubated at this temperature in the calorimeter cell for 12 h. Subsequently, the sample was subjected to a third heating run and the resulting DSC thermogram is shown in Fig. 1g. Clearly, the observed calorimetric endotherm shown in Fig. 1g is virtually identical to that exhibited by the second heating thermogram (Fig. 1f) or the low-temperature endotherm observed in the initial scan (Fig. 1e), indicating that the low-temperature transition is not converted to the high-temperature transition at 2°C within the incubation time of 14 h in the calorimeter. In addition, after a sample was cooled from 55°C to 2°C in the calorimeter, it was incubated at this low temperature for 2 days in the calorimeter. The heating thermogram of this 2-day incubated sample again exhibits only a single endotherm, shown in Fig. 1h, which is virtually indistinguishable from that of Fig. 1f or Fig. 1g. In a separate experiment, a heat-treated sample of *N*-methyl-$diC_{11}PE$ (4 mM) was slowly cooled (0.5 C°/min) from the liquid-crystalline state to 2°C, and then held at 2°C in the cold room for 9 days to allow full equilibration of the *N*-methyl-$diC_{11}PE$ sample in the gel state prior to calorimetry. The heating thermogram of this sample is shown in Fig. 1i; again, it is characterized by a sharp, single endothermic transition centered at 9.0°C. Based on thermograms shown in Figs. 1e–i, one can conclude that the sample of *N*-methyl-$diC_{11}PE$ does not show metastability of the G(II) phase when incubated at 2°C for periods up to 9 days.

It should be emphasized that this series of calorimetric measurements for *N*-methyl-$diC_{11}PE$ were carried out under the experimental conditions similar to those employed for $diC_{11}PE$ dispersions described earlier. The calorimetric results shown in Fig. 1 thus indicate that the phase behavior of these two phospholipids is fundamentally quite different. It should be pointed out that the similar effect of *N*-monomethylation of PE headgroup, which appears to prevent the formation of the high-temperature transition, has been reported by Casal and Mantsch for $diC_{16}PE$ [13]. Since the primary amine group ($-NH_3^+$) in $diC_{11}PE$ is substituted by a *N*-methylated secondary amine group ($-N^+(CH_3)H_2$) in *N*-methyl-$diC_{11}PE$, the very different phase behavior may, therefore, be attributed to the modification of the lipid headgroup.

Quench cooling of $diC_{11}PE$ dispersions

The observation that the second heating thermogram of the $diC_{11}PE$ dispersion exhibits distinctively different endothermic features in comparison with the initial scan, as shown in Figs. 1a and b, indicates that the high-temperature $G(I) \rightarrow L_\alpha$ phase transition with $T_m \simeq 38$°C is irreversible under the experimental conditions. Since the second heating scan is carried out after the sample has been heated above T_m and cooled down slowly from 55°C to 10°C in the calorimeter, it is thus possible that the observed irreversibility of the high-temperature transition may be attributed to the fact that on cooling only a small temperature gradient across the multilamellar liposome exists.

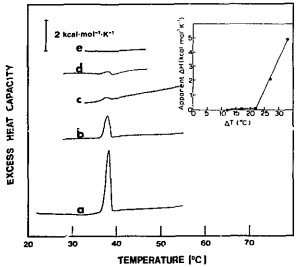

Fig. 2. DSC heating thermograms for heat-treated samples of $diC_{11}PE$. The heat-treated sample was quench cooled (a) from 55 °C to 22 °C; (b) from 55 °C to 28 °C; (c) from 55 °C to 33 °C; (d) from 45 °C to 28 °C; and (e) from 45 °C to 33 °C. The insert shows the apparent transition enthalpy calculated from each of the thermogram versus the temperature gradient (ΔT) with which the quench cooling was carried out. Lipid concentration: 3.04 mM throughout.

In order to examine the effect of temperature gradient across the multilamellar liposome on the reversibility of the high-temperature transition, we have examined the thermotropic phase behavior of quench cooled samples of $diC_{11}PE$. Each sample is quench cooled from 55° or 45 °C to various temperatures between 18 and 38 °C, a temperature range between the low- and high-temperature transitions detected in Figs. 1a and b. The resulting thermograms of these quench cooled $diC_{11}PE$ samples are presented in Fig. 2. Clearly, the G(I) $\rightarrow L_\alpha$ phase transition is detectable in most of the thermograms, indicating that upon quench cooling, some of the liquid-crystalline L_α phase of the heat-treated $diC_{11}PE$ lamellae can be transformed into the G(I) phase. Moreover, the magnitude of the apparent transition enthalpy depends on the temperature gradient with which the quench cooling is carried out as shown in the insert presented in Fig. 2.

Quench supercooling of $diC_{11}PE$ dispersions

In an attempt to investigate the effect of supercooling on the phase behavior of $diC_{11}PE$, we have quench supercooled the heat-treated $diC_{11}PE$ in the liquid-crystalline state to −40 °C. Fig. 3 shows a series of heating thermograms for $diC_{11}PE$ dispersions after supercooling at −40 °C for various time intervals. These representative thermograms are characterized by an exotherm and two endotherms. The transition temperatures of the two endotherms correspond to those of the G(I) $\rightarrow L_\alpha$ and the G(II) $\rightarrow L_\alpha$ transitions as seen in Fig. 1. The apparent transition enthalpies of these endotherms are plotted in Fig. 4 as a function of the −40 °C incubation time. Clearly, the G(I) $\rightarrow L_\alpha$ transition grows nonlinearly with increasing incubation time; the increase in apparent ΔH associated with the G(I) $\rightarrow L_\alpha$ transition is initially more rapid and then asymptotically approaches a limiting value of 12 kcal/mol after 13 days of incubation at −40 °C. Moreover, a relatively large fraction of the L_α phase must have transformed into the G(I) phase during the first incubation hour after quench supercooling at −40 °C, since the thermogram displays a larger high-temperature transition peak (Fig. 3). By contrast, an increase in the incubation time results in a relatively rapid non-linear decrease in the magnitude of the G(II) $\rightarrow L_\alpha$ transition (Figs. 3 and 4), indicating that the G(II) phase of $diC_{11}PE$ in excess water is metastable and that it transforms into the more

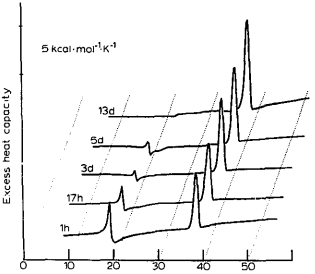

Fig. 3. DSC heating thermograms for $diC_{11}PE$ dispersions after quench supercooling at −40 °C for various time intervals as indicated adjacent to respective thermogram. Lipid concentration: 2.07 mM, 2.46 mM, 2.94 mM, 4.05 mM, and 2.78 mM for 1 h, 17 h, 3 d, 5 d, and 13 d, respectively.

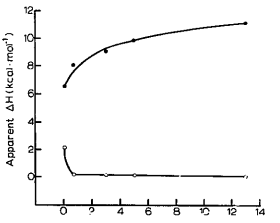

Fig. 4. Apparent transition enthalpies of the two endothermic transitions observed for the quench supercooled $diC_{11}PE$ dispersion versus the incubation time allowed for the dispersions at −40°C. Solid circle (●), apparent ΔH associated with the high-temperature endotherm; open circle (○), apparent ΔH associated with the low-temperature endotherm.

stable G(I) phase at the supercooling temperature of −40°C.

A distinctive feature of the heating thermograms shown in Fig. 3 is the exothermic transition which occurs immediately after the lower temperature endotherm. In fact, DSC experiments indicate that the exothermic transition appears if the heat-treated sample is quench supercooled from 55°C to 10°C or any temperature below 10°C (data not shown). The observation of an exotherm with negative enthalpy suggests that a supercooled metastable (M) state of $diC_{11}PE$ originated from the L_α state is kinetically trapped under the experimental conditions.

Supercooled metastable state

In order to demonstrate that during the exothermic transition the $diC_{11}PE$ in the M state transforms into the G(I) state which subsequently converts to the L_α state within the narrow temperature range of the high-temperature endothermic transition, we have performed additional DSC experiments. First, the heat-treated dispersions of $diC_{11}PE$ were prepared. They were then quench supercooled to −40°C and incubated at that temperature for various times. These −40°C incubated samples should sequentially exhibit an endotherm, an exotherm and an endotherm upon heating continuously to 55°C. A heating scan of the supercooled sample which had been incubated at −40°C for approximately 1 h was initially performed from 0°C to 25°C, a temperature between the exotherm and the high-temperature endotherm. The sample in the calorimeter was held isothermally at 25°C for 1 h. It was then cooled down to 10°C, and was rescanned immediately from 10°C to 55°C. The results are shown in Fig. 5. The first heating scan up to 25°C shows an endotherm centered at 18.1°C followed immediately by an exotherm with the minimum at 19°C (Fig. 5a). A reheating of the sample from 10 to 55°C displays two endotherms with maxima occurring at 18 and 38°C, respectively; in addition, no exotherm at 19°C is observed (Fig. 5b). In a separate DSC experiment, a supercooled sample which had been incubated at −40°C for 3 days was first scanned through the low-temperature endotherm at 18°C and the exotherm at 19°C, and held at 26°C for 1 h (Fig. 5C). It was then cooled to 2°C, and a second heating scan up

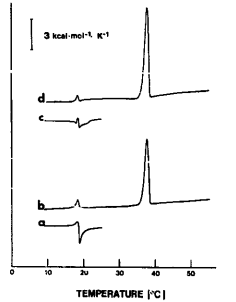

Fig. 5. Successive DSC thermograms of supercooled $diC_{11}PE$ dispersions. (a) Initial heating scan of a supercooled sample which had been incubated at −40°C for 1 h. The heating scan was terminated at 25°C. (b) After incubating at 25°C in the calorimeter for 1 h, the sample was cooled to 10°C and rescanned immediately from 10 to 55°C. (c) Initial heating of a supercooled sample which had been incubated at −40°C for 3 days; the scan was held at 26°C for 1 h. (d) After cooling to 2°C, the sample was rescanned immediately up to 55°C. Lipid concentration: a and b, 2.94 mM; c and d, 2.86 mM.

to 55°C was performed immediately (Fig. 5d). Clearly, the resulting thermograms are similar to the DSC curves shown in Figs. 5a and b. These results suggest that all $diC_{11}PE$ molecules in the M state, irrespective of their thermal history, are converted between 18 and 26°C into the more stable G(I) state which, in turn, undergoes the G(I) → L_α phase transition at 38°C.

^{31}P-NMR studies

Since ^{31}P-NMR is a noninvasive technique which has been successfully employed as a diagnostic tool to ascertain the polymorphic phase behavior of fully hydrated phospholipids [14], we have recorded ^{31}P-NMR spectra for $diC_{11}PE$ dispersions at different temperatures in order to obtain structural information about hydrated $diC_{11}PE$ in excess water.

For heat-treated samples, ^{31}P-NMR spectra of $diC_{11}PE$ were recorded in an ascending temperature mode ranging from 4°C to 60°C. Some of the representative proton-decoupled ^{31}P-NMR spectra are shown in Fig. 6. It is evident that these ^{31}P-NMR spectra exhibit a typical 'bilayer' pattern, which is axially symmetrical with a high-field peak and a low-field shoulder. Negative chemical shift anisotropy ($\Delta\sigma$), determined from the separation between points of maximum slope of the low-field shoulder and of the high-field peak, is plotted in Fig. 7. The value of $\Delta\sigma$ is observed to decrease gradually with increasing temperature up to 17°C. From 17° to 18°C, $\Delta\sigma$ decreases abruptly to a lower value; thereafter, $\Delta\sigma$ remains relatively constant at higher temperatures. This abrupt decrease in $\Delta\sigma$ can be attributed to a substantial increase in rotational motion of the phosphate moiety in the lipid headgroup, and such an additional motion represents one of the characteristics of phospholipid dynamics in the liquid-crystalline (L_α) state [15]. The ^{31}P-NMR data thus indicate that $diC_{11}PE$ molecules in the heat-treated sample are packed in lamellar structures which undergo a gel → liquid-crystalline phase transition between 17°C and 18°C; hence, the observed phase transition for the heat-treated sample based on ^{31}P-NMR data is compatible with the G(II) → L_α transition detected by DSC for heat-treated samples of $diC_{11}PE$ (Fig. 1b), although the transition temperature associated

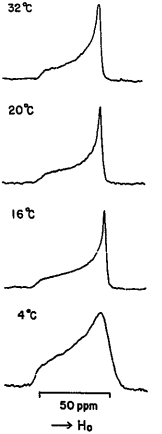

Fig. 6. Proton noise-decoupled 121 MHz ^{31}P-NMR spectra of the heat-treated sample of $diC_{11}PE$. The spectra were collected typically from 8000 to 10000 scans for each spectrum and were recorded in an ascending temperature mode at indicated temperatures.

with the marked lowering of $\Delta\sigma$ in ^{31}P spectra is about 1 C° smaller than the value of T_m determined by DSC.

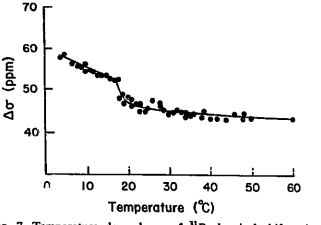

Fig. 7. Temperature dependence of ^{31}P chemical shift anisotropy (in ppm) for the heat-treated sample of $diC_{11}PE$.

For nonheated samples of $diC_{11}PE$ at temperatures below 36°C, Fourier transformation of data sets consisting of 10000 scans did not result in detectable ^{31}P-NMR signals. Data sets of 36000 repeated scans resulted in ^{31}P-NMR spectra with poor signal to noise and without any discernible spectral features. By contrast, when temperature of the sample was raised to 36°C, subsequent ^{31}P-NMR spectra with excellent signal to noise were collected typically from 8000–10000 scans for each spectrum. The lineshapes of these spectra are 'bilayer' pattern, and the negative chemical shift anisotropies exhibit a small but linear dependence of temperatures ranging from 36°C to 50°C, with an averaged value of 44.7 ± 0.5 ppm. These characteristics are identical to those exhibited by heat-treated sample at corresponding temperatures as shown in Figs. 6 and 7. The detection of axially symmetric ^{31}P-NMR spectra from 8000–10000 scans at temperatures only above 36°C suggests that the phosphate moiety of $diC_{11}PE$ in the nonheated sample is severely immobilized at $T < 36$°C, and the severe motional restriction is abruptly relaxed upon heating the sample across a small temperature range (< 2°C) immediately above 36°C. Furthermore, ^{31}P data indicate that at $T > 36$°C $diC_{11}PE$ molecules are packed in a lamellar structure with liquid-crystalline characteristics. Thus, the ^{31}P-NMR spectral change observed between 36 and 38°C is consistent with the $G(I) \rightarrow L_\alpha$ phase transition detected by DSC for the nonheated sample of $diC_{11}PE$ as seen in Fig. 1a. However, the transition temperature at which a constant axially symmetric ^{31}P-NMR spectrum occurs is slightly lower than that of the $G(I) \rightarrow L_\alpha$ phase transition determined more accurately by DSC.

Discussion

$DiC_{12}PE$ is the first species of saturated diacyl phosphatidylethanolamine which has been extensively studied by a wide variety of biophysical techniques [1–6]. The nonheated sample of $diC_{12}PE$ displays a highly cooperative endothermic transition at 44.85°C by DSC, whereas a second immediate heating scan of the same sample after cooling from the liquid-crystalline state exhibits a smaller endothermic transition with a downshift in T_m by about 15°C. Based on FT-infrared and X-ray diffraction data [1–3], the high-temperature transition has been assigned to the $L_c \rightarrow L_\alpha$ phase transition, where the L_c state is a crystalline-like phase with the hydrocarbon chains of $diC_{12}PEs$ packed in a highly ordered subcell lattice. The low-temperature transition, on the other hand, corresponds to the $L_\beta \rightarrow L_\alpha$ phase transition, where the L_β state is a gel-like phase in which acyl chains in an all *trans* conformation are packed in a less ordered subcell lattice.

We have detected two endothermic transitions for samples of $diC_{11}PE$ in excess water; the magnitude of each transition depends on the thermal history of the sample (Fig. 1a–d). The transition entropies for the high-temperature and low-temperature transitions can be calculated, based on values of ΔH and T_m obtained from Fig. 1a and b, to be 44.81 and 9.80 e.u./mol, respectively. Since transition entropy (ΔS) is a measure of the total entropy change of the phospholipid bilayer which undergoes a phase transition at T_m, the magnitude of ΔS can thus be related to the overall change in inter- and intra-chain configuration entropies which, in turn, can be correlated to the difference in acyl chain packing in bilayers at states immediately above and below T_m [16]. If we assume that the acyl chain packings of $diC_{11}PEs$ in the two liquid-crystalline states (L_α) immediately above the T_m of the $G(I) \rightarrow L_\alpha$ and $G(II) \rightarrow L_\alpha$ phase transitions are virtually identical, then the calculated transition entropies of 44.81 and 9.80 e.u./mol at the transition temperature for the $G(I) \rightarrow L_\alpha$ and $G(II) \rightarrow L_\alpha$ transitions suggest strongly that the acyl chain packings of lamellar lipids in the G(I) state near T_m are significantly more ordered than those in the G(II) state near T_m. The thermodynamic data can, therefore, be taken to imply that the magnitudes of the chain-chain van der Waals interactions for $diC_{11}PE$ bilayers in the G(I) phase are significantly larger than those in the G(II) phase at the corresponding reduced temperature. Hence, our thermodynamic analysis together with the known phase structures of $diC_{12}PE$ lamellae discussed earlier enable us to conclude that the $G(I) \rightarrow L_\alpha$ and $G(II) \rightarrow L_\alpha$ phase transitions observed for $diC_{11}PE$ appear to correspond to the $L_c \rightarrow L_\alpha$ and $L_\beta \rightarrow L_\alpha$ transitions, respectively, for $diC_{12}PE$, and that the G(I) and

G(II) states can be suggested as the L_c and L_β phases, respectively.

The appearance of the G(I) → L_α phase transition for samples of $diC_{11}PE$ which have been first heated above T_m and then quench cooled to a temperature between 18 and 38°C prior to the DSC heating scan depends on the temperature gradient with which the quench cooling is carried out. Results shown in Fig. 2 indicate that a G(I) → L_α phase transition is clearly discernible for heat-treated samples of $diC_{11}PE$ provided the temperature gradient used for quench cooling is greater than 22°C. This observation is of considerable interest since it provided the first evidence of the fact that the G(I) → L_α phase transition of PE can be reverted by temperature gradient. It also indicates that lamellar $diC_{11}PE$ in the liquid-crystalline state can be metastable below 38°C under certain experimental conditions.

An interesting phase transition detected for $diC_{11}PE$ is the exotherm which occurs immediately following the low-temperature endotherm as shown in Fig. 3. It should be emphasized that this exotherm is observed in the heating run only after the $diC_{11}PE$ sample has been quench supercooled and held at the supercooled temperature for 1 h or longer. A possible explanation for observing this exotherm is to attribute the exothermic transition to a L_α → G(I) phase transition. It is possible that after quench supercooling, a significant amount of $diC_{11}PE$ sample is already transformed into the G(I) phase, while the remaining is in the G(II) phase. On heating slowly through the low-temperature endotherm at 18°C, the G(II) phase is converted into a liquid-crystalline phase (L_α) which, in the presence of the preexisting G(I) phase, converts immediately to the stable, ordered G(I) phase exothermally at about 19°C. A very similar explanation has, in fact, been proposed for the exothermic transition observed at 72°C for *N*-lignocerylgalactosylsphingosine bilayers [17]. However, it is difficult to understand why, if a G(I) phase induced nucleation is indeed involved, the slowly cooled $diC_{11}PE$ bilayer carried out under various conditions does not display calorimetrically the exothermic trough upon slow heating as shown in Fig. 1c and d and Fig. 5b and d. A perhaps more plausible explanation is that the exotherm corresponds to the M → G(I) phase transition, where M is a metastable phase formed kinetically from the L_α phase upon quench supercooling of the lipid sample. If this conjecture is reasonable, then the supercooled metastable M state can be related to all other states of $diC_{11}PE$ as indicated in Scheme I.

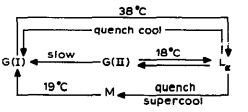

Scheme I. Metastable M state and phase transitions.

The molecular structure of lamellar $diC_{11}PE$ in the G(I) state is comparable to that of $diC_{12}PE$ in the crystalline state as discussed earlier. In the crystalline state, interbilayer hydrogen bonding interactions are most likely to occur between the phosphate and amine groups [18]. Recently, X-ray diffraction studies of $diC_{12}PE$ indicate that the interstitial water space between adjacent bilayers of $diC_{12}PE$ is very small; this small interstitial space may arise from interbilayer hydrogen bond formation or electrostatic interactions between the amine and phosphate groups on opposing bilayers [19]. Our ^{31}P-NMR spectra indicate that $diC_{11}PE$ molecules in the nonheated sample are highly immobilized at $T < 36$°C; this immobilization can be interpreted in light of the recent X-ray diffraction data as a result of headgroup-headgroup interactions of PEs across the interstitial space between lipid lamellae. A schematic representation of the bilayer in the G(I) state is shown in Fig. 8.

The molecular structure of $diC_{11}PE$ lamellae in the M state is not known. However, the M → G(I) phase transition is exothermic. This means that packing of the acyl chains of $diC_{11}PE$ in the M state is more disordered than that in the G(I) state. This information plus the fact that the M state is transformed from the L_α state upon quick supercooling lead us to speculate that a prime candidate for the molecular structure of $diC_{11}PE$ lamellae in the M state is the one schematically illustrated in Fig. 8. This model shows basically two characteristic features. First, the supercooled metastable M state is a multilamellar structure with melted acyl chains. This is consistent with the

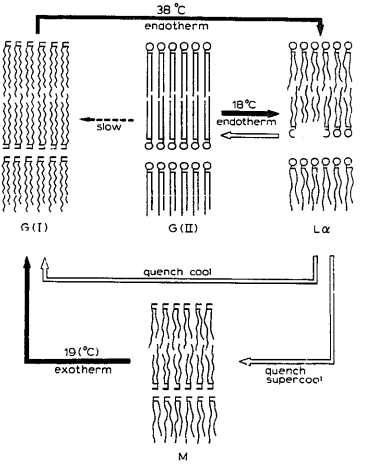

Fig. 8. Schematic drawings to illustrate the various states of different lamellar structure in $diC_{11}PE$. The stable G(I) crystalline phase is represented with acyl chains having zig-zag carbon-carbon backbones, and static headgroups with a minimal interbilayer aqueous space. The G(II) gel phase is represented with straight acyl chains, spherical headgroups (indicating rotational motions of the headgroup), and a large interbilayer aqueous space. The liquid-crystalline L_α phase is represented with highly disordered acyl chains and a large interbilayer aqueous space. The supercooled metastable M state is hypothesized to be a multilamellar system with disordered acyl chains. However, the headgroup conformation and the interbilayer aqueous space are similar to those of the G(I) state. Hence, interbilayer headgroup-headgroup interactions are likely to occur in the M state. Solid arrows indicate the conversion of the lipid state on heating; open arrow represents the conversion on cooling; dotted arrow represents the slow conversion at low temperatures ($< 10\,^\circ C$).

observed exothermic transition. Second, the interstitial aqueous space between adjacent bilayers is assumed to be very small. This feature is discussed in more detail in the following section.

When the dipalmitoylphosphatidylcholine bilayer undergoes the $L_{\beta'} \rightarrow L_c$ phase transition, headgroup dehydration and acyl chain ordering are known to be associated with the phase transition; moreover, the headgroup dehydration is demonstrated to be the rate-limiting step in the L_c phase formation [20]. It is thus reasonable to assume that in the time course of the $L_\alpha \rightarrow M + G(I) + G(II)$ phase transformations for $diC_{11}PE$ upon quick supercooling, headgroup dehydration and acyl chain ordering are also occurring simultaneously; however, the onset and the rate of each of the processes do not take place in a completely synchronized manner. In fact, the first structural feature discussed in the preceding section demands that the acyl chain ordering be lingering, at least initially, behind headgroup dehydration upon quick supercooling. Clearly, $diC_{11}PE$ lamellae in this initial lag phase must have reduced interstitial aqueous space between adjacent bilayers due to headgroup dehydration. In addition, the bilayer will also have melted acyl chains, because the acyl

chain ordering has not yet begun to occur in this initial lag phase. This $diC_{11}PE$ lamellar structure occurring only in the transient lag phase is that which we propose to be the M state.

In the M state, interbilayer headgroup-headgroup interactions across the small interstitial space probably can take place. Perhaps, the interbilayer headgroup-headgroup interaction tends to promote the conversion of the melted acyl chains of $diC_{11}PE$ to the highly ordered chain-packing mode at 19°C, leading to the exothermic M → G(I) phase transition as shown in Fig. 8. In Fig. 8, the well-known structures of G(II) or L_β and L_α states are also diagrammatically presented.

The metastability of the G(II) state can be most appropriately described in terms of dehydration. After prolonged incubation of G(II) state bilayers at 2°C, some of the bound water molecules packed around the lipid headgroup are probably released into the bulk water due to the ability of the lipid headgroup in one bilayer to involve in the hydrogen bond formation and the electrostatic interaction with the headgroup of another lipid molecule in the opposing bilayer. This interbilayer headgroup-headgroup interaction at low temperatures will undoubtedly damp the amplitude and rate of acyl chain reorientation fluctuations about the long molecular axis; the effect is to transform the acyl chain packing into a highly ordered mode. The gradual dehydration of $diC_{11}PE$ headgroup at low temperature thus results in a slow conversion of the lipid in the G(II) state to the more stable G(I) state, as schematically shown in Fig. 8.

Based on steric considerations, one would expect that the headgroup-headgroup interaction across the adjacent bilayers will be weakened appreciably by monomethylation of the amine group in $diC_{11}PE$. The observed phase behavior of *N*-methyl-$diC_{11}PE$ shown in Fig. 1 indeed supports the proposed interbilayer headgroup-headgroup interaction. For instance, the small magnitude of the high-temperature transition observed for non-heated sample of *N*-methyl-$diC_{11}PE$, Fig. 1e, is consistent with the notion that the presence of a *N*-monomethyl moiety in the lipid headgroup decreases substantially the headgroup-headgroup interaction across the adjacent bilayers. Also, because of the steric hindrance imposed by the *N*-monomethyl group, a close contact between the adjacent lamellae is configurationally more difficult; consequently, a reconversion of the low-temperature transition to the high-temperature transition for the heat-treated sample would seem to be highly improbable. Indeed, this is congruent with our DSC data on the heat-treated sample of *N*-methyl-$diC_{11}PE$ which fails to show the conversion of the bilayer from the less stable G(II) form to the more stable G(I) form after prolonged incubation up to 9 days at 2°C (Figs. 1f–i). The disappearance of gel state metastability by monomethylating the amine group in PE can thus be qualitatively interpreted as due to the substitution of the headgroup-headgroup interaction in PEs across the adjacent lamellae by the headgroup-H_2O interaction in *N*-methyl-PEs. Finally, we would like to emphasize that the lipid headgroup is functionally able to modulate the hydration/dehydration of lipid bilayers, and that the headgroup-headgroup interaction across the interbilayer space may affect directly the structural and phase behavior of bilayer membranes.

Acknowledgements

This work was supported, in part, by U.S. Public Health Service Grant GM-17452 from the National Institutes of General Medical Sciences, NIH, Department of Health and Human Services.

References

1 Chang, H. and Epand, R.M. (1983) Biochim. Biophys. Acta 728, 319–324.
2 Mantsch, H.H., Hsi, S.C., Butler, K.W. and Cameron, D.G. (1983) Biochim. Biophys. Acta 728, 325–330.
3 Seddon, J.M., Harlos, K. and Marsh, D. (1983) J. Biol. Chem. 258, 3850–3854.
4 Chowdhry, B.Z., Lipka, G., Dalziel, A.W. and Stuttevant, J.M. (1984) Biophys. J. 45, 901–904.
5 Mulukutla, S. and Shipley, G.G. (1984) Biochemistry 23, 2514–2519.
6 Finegold, L., Melnick, S.J. and Singer, M.A. (1985) Chem. Phys. Lipids 38, 387–390.
7 Gagné, J., Stamatatos, L., Diacovo, T., Hui, S.W., Yeagle, P.L. and Silvius, J.R. (1985) Biochemistry 24, 4400–4408.
8 Comfurius, P. and Zwaal, R.F.A. (1977) Biochim. Biophys. Acta 488, 36–42.
9 Gomori, G. (1942) J. Lab. Clin. Med. 27, 955–958.
10 Xu, H. and Huang, C. (1987) Biochemistry 26, 1036–1043.
11 Rance, M. and Byrd, R.A. (1983) J. Magn. Res. 52, 221–240.
12 Shaka, A.J., Keeler, J. and Freeman, R. (1983) J. Magn. Res. 53, 313–340.

13 Casal, H.L. and Mantsch, H.H. (1983) Biochim. Biophys. Acta 735, 387–396.
14 Smith, I.C.P. and Ekiel, I.H. (1984) in Phosphorus-31 NMR: Principles and Applications (Gorenstein, D.G., ed.), pp. 447–475, Academic Press, New York.
15 Griffin, R.G., Powers, L. and Pershan, P.S. (1978) Biochemistry 17, 2718–2722.
16 Huang, C., Lapides, J.R. and Levin, I.W. (1982) J. Am. Chem. Soc. 104, 5926–5930.
17 Reed, R.A. and Shipley, G.G. (1987) Biochim. Biophys. Acta 896, 153–64.
18 Boggs, J.M. (1987) Biochim. Biophys. Acta 906, 353–404.
19 McIntosh, T.J. and Simon, S.A. (1986) Biochemistry 25, 4948–4952.
20 Wu, W., Chong, P.L.-G. and Huang, C. (1985) Biophys. J. 47, 237–242.